Paper: Dr4-2-3680; 2009/4/13

Integrated Ground Motion and Tsunami Simulation for the 1944 Tonankai Earthquake Using High-Performance Supercomputers

Takashi Furumura and Tatsuhiko Saito

Center for Integrated Disaster Information Research, Interfaculty Graduate
School of Interdisciplinary Information Studies, The University of Tokyo
1-1-1 Yayoi, Bunkyo-ku, Tokyo 113-0032, Japan
E-mail: {furumura, saito-ta}@eri.u-tokyo.ac.jp
[Received December 23, 2009; accepted February 4, 2009]

An integrated simulation of seismic wave and tsunami has been developed for mitigation of earthquake and tsunami disasters associated with large subduction-zone earthquakes occurring in the Nankai Trough. The ground motion due to the earthquake is firstly calculated by solving equation of motions with heterogeneous source-rupture model and 3-D heterogeneous subsurface structural model. Tsunami generation and propagation in heterogeneous bathymetry is then simulated by solving the 3-D Navier-Stokes equation. Ground motion and tsunami simulations are combined through an appropriate dynamic boundary condition at the sea floor. Thanks to supercomputers and efficient parallel computing, we are reproducing strong ground motion and tsunamis caused by the M8.0 Tonankai earthquake in the Nankai Trough in 1944. The visualized seismic wavefield and tsunami derived by integrated simulation provides a direct understanding of disasters associated with Nankai Trough earthquakes with the development of long-period ground motion in highly populated basins such as Tokyo, Osaka, and Nagoya and tsunamis striking along Japan's Pacific Ocean coast.

Keywords: Nankai-Trough earthquake, strong ground motion, tsunami, Earth Simulator, long-period ground motions, 1944 Tonankai earthquake

1. Introduction

Large magnitude (M)-8 earthquakes have repeatedly occurred in the Nankai Trough every 100-200 years. Strong ground motion and tsunamis due to the 1944 M8.0 Tonankai and 1946 M8.0 Nankai earthquakes seriously damaged areas from Kyushu to Tokai, killing over 2,500 persons in total. Over 60 years have been passed since these events, so the next Nankai Trough earthquake is predicted to occur within the next 30 years.

To better understand and mitigate earthquake and tsunami disasters from such earthquakes, we must be able to realistically simulate these phenomena by employing supercomputers to calculate equation of motion that describe seismic wave propagation and the Navier-Stokes (N-S) equation that describe water flow with detailed source-rupture models, high-density three-dimensional (3-D) subsurface structural models, and high-resolution bathymetry data.

The dynamic seafloor displacement due to the earthquake causes an initial tsunami on the sea surface above the source area. However, ground-motion and tsunami simulations are conducted independently using different source and structural models even though they are relating very closely. Current tsunami simulations are often based on approximation equations such as linear long-wave theory (LLW) rather than directly solving N-S equations. For these reasons, understanding of strong ground motion and tsunamis associated with the Nankai-Trough earthquakes remains insufficient.

Therefore, we have developed an integration simulation model combining ground motion and tsunami simulation that accurately represents strong ground motion and tsunamis caused by the Nankai Trough earthquakes. In this integrated simulation, the ground motion and tsunami due to heterogeneous source-rupture process and propagating in 3-D subsurface structure can be simulated consistently. Such coupled ground motion and tsunami simulation was developed and first applied to 1993 M7.8 Hokkaido-Nansei Oki earthquake simulation by Ohmachi et al. (2001) [1], who used the boundary element method (BEM) for calculating dynamic seabed displacement caused by complex fault-rupture in a homogeneous half-space subsurface structure, then tsunami simulation was conducted by solving the N-S equation in 3-D based on the finite-difference method (FDM). Following this pioneering study, we developed an alternative integrated simulation model using a realistic 3-D heterogeneous subsurface structure model and high-resolution bathymetric data by efficient large-scale parallel simulation using supercomputers. We calculate dynamic ground displacement and coseismic seafloor deformation by FDM simulation of equations of motion in 3-D. Then, the results of seafloor ground motion are used for tsunami generation and propagation simulation as an input in the FDM simulation of 3-D N-S equations.

In the present paper we introduce the integrated FDM simulation of ground motion and tsunami and their effectiveness of parallel computing in large-scale simulation using the Earth Simulator at the Japan Marine Sciences and Technology Center and the T2K Open Supercomputer at the Information Technology Center of the University of Tokyo. We applied the integrated simulation to the 1944 M8.0 Tonankai earthquake, demonstrating the developments of the long-period ground motions and tsunami from the Nankai-Trough earthquake. The visualization of ground motion and tsunami using a 3-D visualization technique developed by Furumura et al. (2003) [2] provides a direct understanding of development and propagation properties of long-period ground motion occurring in populated cities and long-time duration of coastal tsunamis.

2. 1944 Tonankai Earthquake Ground Motion Simulation

Ground motion and coseismic deformation due to earthquake fault ruptures in 3-D heterogeneous structures are evaluated by the 3-D FDM simulation of equations of motion expressed in 3-D Cartesian coordinates system as follows:

$$\begin{aligned} \rho\,\ddot{u}_x &= \frac{\partial\sigma_{xx}}{\partial x}+\frac{\partial\sigma_{xy}}{\partial y}+\frac{\partial\sigma_{xz}}{\partial z}+f_x,\\ \rho\,\ddot{u}_y &= \frac{\partial\sigma_{yx}}{\partial x}+\frac{\partial\sigma_{yy}}{\partial y}+\frac{\partial\sigma_{yz}}{\partial z}+f_y, \qquad (1)\\ \rho\,\ddot{u}_z &= \frac{\partial\sigma_{zx}}{\partial x}+\frac{\partial\sigma_{zy}}{\partial y}+\frac{\partial\sigma_{zz}}{\partial z}+f_z, \end{aligned}$$

where σ_{pq} , f_p, and ρ are stress, body force, and density and $\ddot{u}_p\,(p=x,y,z)$ represents particle acceleration. Stress components in an isotropic elastic medium are given by:

$$\begin{aligned} \sigma_{pq} &= \lambda(e_{xx}+e_{yy}+e_{zz})\delta_{pq}+2\mu\, e_{pq},\\ &\quad (p,q)=(x,y,z), \qquad (2) \end{aligned}$$

with Lame's constants λ and μ, and δ_{pq} is the Kronecker delta. Strains are defined by:

$$e_{pq}=\frac{1}{2}\left(\frac{\partial u_p}{\partial q}+\frac{\partial u_q}{\partial p}\right),\quad (p,q=x,y,z). \qquad (3)$$

Eqs. (1)-(3) are solved explicitly by FDM simulation using a staggered-grid model (Graves, 1996 [3]) with suitable absorbtion boundary conditions at the edge of the model to minimize artificial reflection (Cerjan et al. 1985 [4]). A zero-stress boundary condition (Graves, 1996 [3]) is applied at the surface. Sea water is simply introduced in the simulation model by assigning elastic constants $\mu=0$ and density $\rho=1.0$ g/cm^3 to the water column cell. Anelastic properties (Q_p,Q_s) are implemented in FDM simulation by applying appropriate damping coefficients to velocity and stress components in each time step (Graves, 1996 [3]).

3-D simulation model is discretized by a small mesh, and elastic and anelastic parameters are assigned to each mesh to represent the heterogeneous subsurface structure. The seismic fault source is represented by a number of equivalent body forces that assigned on the fault plane. Each point source radiates a seismic wave of assumed source-time functions when the fault rupture passes over each point. The mesh size of the FDM simulation and interval of body forces should be smaller than the minimum wavelength of seismic waves appearing in the simulation. A smaller mesh is also required for modeling high-resolution subsurface structures and the source-rupture model in FDM simulation.

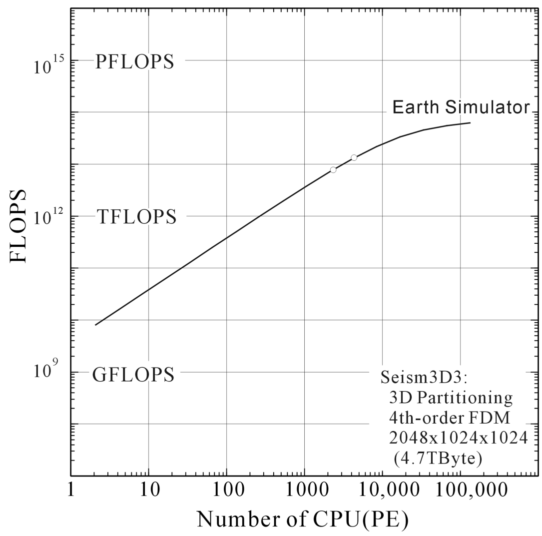

Fig. 1. Estimated computational speed in FLOPS for parallel FDM simulation of seismic waves using the Earth Simulator. Open circles: observed speed, and solid line: anticipated speed, as functions of CPU (PE) numbers.

2.1. Parallel FDM Ground Motion Simulation

To conduct large-scale, high-resolution simulation of seismic waves by solving equations of motions, we developed parallel 3-D FDM (Furumura and Chen, 2004 [5]) based on a domain-partitioned procedure. The 3-D model is partitioned into subregions allocated to many processors for concurrent computing, and a message-passing interface (MPI) is used for exchanging data between neighbor regions in each time step.

The speed-up of parallel FDM simulation of a seismic wave is shown in **Fig. 1** as a number of processor (PE) of the Earth Simulator (ES) increases. The FDM simulation model has 2048 × 1024 × 1024 grid points and a staggered-grid fourth-order FDM is used for calculating space and 2$^{\mathrm{nd}}$-order for time derivatives in the equation of motion. Computer time was measured for parallel computing using 2048 and 4096 PE of the ES (open circles, **Fig. 1**), and the theoretical speed-up rate using from 2 to 10,000 PEs is expected based on the Amdahl's law (solid line, **Fig. 1**). Results shows fairly good speed-up by parallel computing using more than 10,000 PEs. The FDM ground motion simulation extracts good vector computing hardware performance (Furumura and Chen, 2004 [5]) on the ES, and the estimated FDM computing performance is 4.8 GFLOPS for each PE, or 60% of the peak performance of the processors at 8 GFLOPS/PE.

2.2. Simulation Model

We used the parallel FDM simulation of ground motion implemented on the ES for calculating ground motion for the 1944 Tonankai earthquake. The simulation

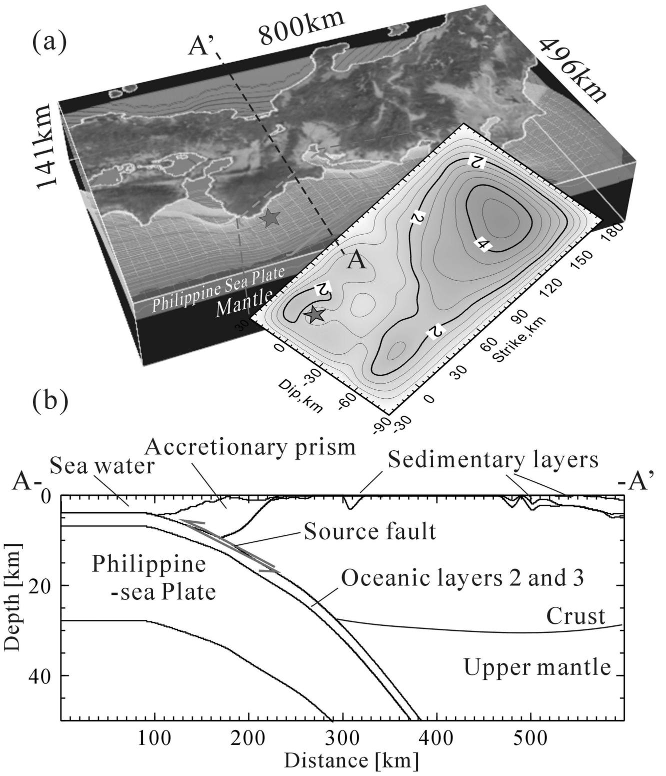

Fig. 2. (a) 3-D subsurface structure model of the Nankai trough and western to central Japan and slip distribution (m) in the fault model of the 1944 Tonankai earthquake used in FDM simulation of seismic wave propagation. (b) Vertical profile of the structure along line A-A'.

model covers 496 × 800 km and extends 141 km deep, which has been discretized using a uniform mesh of 0.4 × 0.4 × 0.2 km (**Fig. 2**). A structural model of the Earth's crust and upper-mantle beneath central Japan is constructed based on the model of sedimentary structures (Tanaka et al., 2006 [6]) and the shape of the subducting Philippine-Sea Plate. Both are constructed by based on reflection and refraction experiments, deep land drilling, and gravity data (Baba et al., 2006 [7]).

The near-surface sedimentary structure has three layers; $V_s = 0.5$, 0.9, and 1.5 km/s for S wave; $V_p = 1.8$, 2.3, and 3.0 km/s for P wave, overlying rigid bedrock of $V_s = 3.2$ km/s and $V_p = 5.5$ km/s (Tanaka et al., 2006 [6]). Physical parameters of P- and S-wave speed (V_p, V_s), density (ρ), and attenuation coefficients for P- and S-wave (Q_p, Q_s) for the crust, upper mantle, and subducting Philippine-Sea Plate are used in the model following the previous study (Furumura et al., 2008 [8]). Our simulation treats seismic waves with periods over $T > 2$ s with a minimum sampling of 2.5 grid points per shortest wavelength of the seismic wave field.

The source-slip model for the 1944 Tonankai earthquake is derived by an inversion using a near-field strong motion waveform (Yamanaka, 2004 [9]). The inferred fault model is 180 × 90 km, and maximum slip of 4 m radiates seismic waves with a total seismic moment of $M_o = 1.0*10^{21}$ Nm ($M_w = 8.0$) (**Fig. 2**). The fault source is resampled in 2 × 2 km segments. Equivalent body forces for double-couple sources and a triangular slip-velocity function with a pulse width of $T = 2$ s are assumed over the fault plane above the interface of the subducting Philippine-Sea Plate at a dipping angle of about 9 deg. The fault rupture spreads over the fault plane from the hypocenter at an average rupture speed of $V_r = 2.95$ km/s.

2.3. Simulation Results

The results of the FDM simulation for the seismic wave propagation from the 1944 Tonankai earthquake demonstrate the strength of horizontal velocity ground motion at time $T = 15$ s, 40 s, 90 s, and 120 s from when the earthquake begins (**Fig. 3**). A sequence of snapshots clearly shows the spread of seismic waves from the source fault where the fault ruptures spreading from southwest to northeast at a speed slightly less than S-wave speed.

The development of the long-period ground motion at a period of $T = 3$-6 s is clear developed at the rupture front due to the directivity of the rupturing fault. Later time frames ($T = 90$ s and 120 s) capturing significant amplification of long-period ground motion in large sedimentary basins such as those beneath Osaka, Nagoya, and Tokyo, where thick sedimentary rocks of over $h = 3000$ m cover rigid bedrock.

The strong motion record during the 1944 Tonankai earthquake was well documented by strong-motion instruments at Yokohama, Tokyo, and Chiba despite recordings being clipped completely near the source area such as at Nagoya, Shizuoka, and Mishima. An example of a smoke-paper strong-motion seismograph at central Tokyo (Otemachi) recorded by strong motion instruments of the Central Meteorological Observatory is displayed in **Fig. 4 (a)**. The digitized dataset of original seismographs was corrected for pen-arc and base-line errors and the instrumental response to obtain actual ground motion (Furumura and Nakamura, 2006 [10]; **Fig. 4 (b)**). Long-period ground motion observed in Tokyo demonstrated very large >10 cm/s, prolonged >10 min long-period ground shaking at a dominant period of $T = 8$ s. Such long-period ground motion developed in Tokyo caused by future Nankai Trough earthquakes is expected to cause serious impact on modern, large-scale structures such as high-rise buildings, oil storage tanks, and long bridges. Such long-period constructions did not exist during the previous earthquakes that occurred more than 60 years ago.

In comparing simulated waveforms of north-to-south component ground velocity motion (**Fig. 4 (b)**), finding that simulation results reproduced major features of observed ground motion of long-period signals developed by the 1944 Tonankai earthquake very well. The velocity response spectrum of simulated and observed ground motion of horizontal motion (**Fig. 4 (c)**) also showed the effectiveness of our simulation model in simulating long-period ground motion over $T > 2$ s.

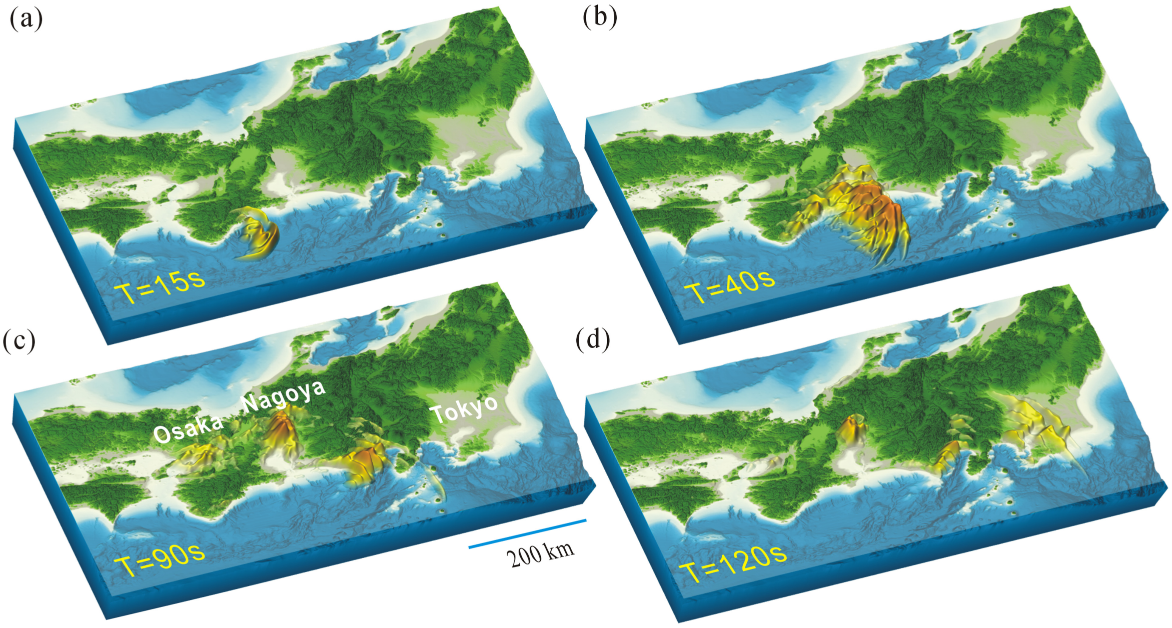

Fig. 3. Snapshots of seismic wave propagation derived using 3-D FDM simulation for the 1944 Tonankai earthquake for (a) T = 15, (b) 40 s, (c) 90 s, and (d) 120 s after when the earthquake began.

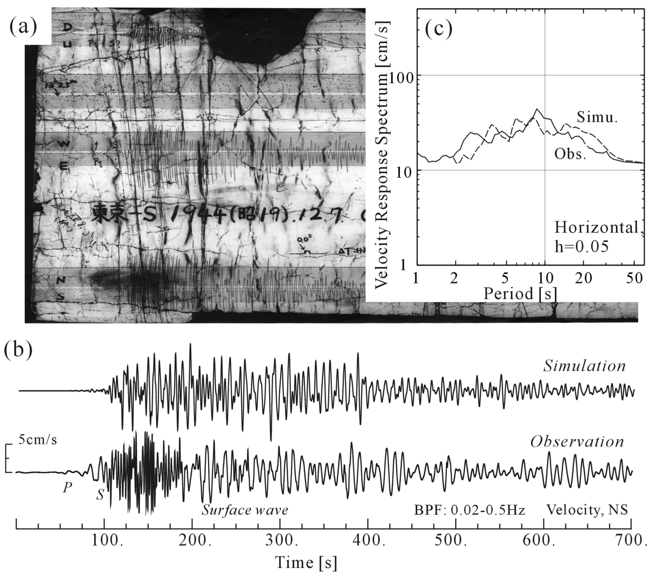

Fig. 4. (a) Smoked-paper seismogram recorded at Tokyo during the 1944 Tonankai earthquake. (b) Comparison of simulation (top) and observed waveform data (bottom) in NS-component ground velocity motion. (c) Velocity response spectra of horizontal motion derived in simulation (dashed line) and observation (solid line).

3. 1944 Tonankai Earthquake Tsunami Simulation

We used ground motion simulations results in dynamic seafloor movement caused by the 1944 Tonankai earthquake in tsunami generation and propagation simulation which is described by 3-D N-S equations for incompressible flow.

In Cartesian coordinates (x,y,z), with z the vertical axis, the N-S equation is written as follows:

$$\begin{cases} \frac{\partial u}{\partial t}+u\frac{\partial u}{\partial x}+v\frac{\partial u}{\partial y}+w\frac{\partial u}{\partial z}=-\frac{\partial}{\partial x}\left(\frac{p}{\rho_0}\right)+\nu\nabla^2 u, \\ \frac{\partial v}{\partial t}+u\frac{\partial v}{\partial x}+v\frac{\partial v}{\partial y}+w\frac{\partial v}{\partial z}=-\frac{\partial}{\partial y}\left(\frac{p}{\rho_0}\right)+\nu\nabla^2 v, \\ \frac{\partial w}{\partial t}+u\frac{\partial w}{\partial x}+v\frac{\partial w}{\partial y}+w\frac{\partial w}{\partial z}=-\frac{\partial}{\partial z}\left(\frac{p}{\rho_0}\right)+\nu\nabla^2 w+g, \end{cases} \quad (4)$$

where u, v, and w are velocity components along the x, y, and z-axes, p is pressure, g acceleration due to gravity, ρ_o density, and ν the kinematic viscosity coefficient for sea water ($\nu = 10^{-6}$ m^2/s). A hydrostatic pressure field is assumed at the initial condition for p, represented by linearly increasing pressure with depth from the sea surface to the sea bottom as:

$$p(z)=\begin{cases} 0 & \text{for} \quad z \geq H_0 \\ -g(H_0-z) & \text{for} \quad z < H_0. \end{cases} \quad (5)$$

Kinematic boundary conditions at the sea surface for $z = h_s(x,y,t) = H_0(x,y)+\eta(x,y,t)$ are given by:

$$\frac{\partial\eta}{\partial t}+u\frac{\partial\eta}{\partial x}+v\frac{\partial\eta}{\partial y}=w, \quad (6)$$

where H_0 is sea depth and η is tsunami height at time t. Our simulation treats offshore tsunamis because the boundary condition (6) on the sea surface cannot account for tsunami wavefront breaking and tsunami run-up.

To solve Eqs. (4) and (6), we use the conventional SOLA technique developed by Hirt et al. (1975) [11], which has been widely used for simulating flow of fluid in 3-D. In simulation, velocities and pressure components in cells on the staggered-grid are updated iteratively at each time step to satisfy the following continuity conditions for incompressible fluid at a satisfactory level (err $< 10^{-6}$) as follows:

$$\frac{\partial u}{\partial x}+\frac{\partial v}{\partial y}+\frac{\partial w}{\partial z}=0. \quad \quad (7)$$

The dynamic vertical seafloor movement on the sea floor $\dot{u}_z(x,y,t)$ derived by the simulation of ground motion is introduced into the tsunami simulation, with the velocity boundary condition at the seafloor during source rupture time $t \leq t_s$ as:

$$w(x,y,h_b(x,y)) = \begin{cases} \dot{u}_z(x,y,t) & for \quad 0<t \leq t_s, \\ 0, & for \quad t>t_s, \end{cases} \quad (8)$$

where $z = h_b(x,y)$ represents seafloor depth distribution. The vertical flow of water due to seafloor movement above the source region lifts the sea surface, which is the initial tsunami developed by the earthquake.

The developed initial tsunami distribution at the sea surface is usually smoother than the shape of coseismic seafloor deformation caused by the earthquake because a thick cover of seawater and finite source-duration time works as a sort of high-cut filter to remove large-wave number components from the shape of initial tsunami developed at sea surface (Kajiura, 1963 [12], Saito and Furumura, 2009 [13]). As time increases, initial tsunami distribution gradually spreads away from the source region as a gravity wave. As the tsunami propagates long distances in deep and heterogeneous bathymetry, initial tsunami shape is distorted significantly due to dispersion (Shigihara and Fujima 2006 [14]) and scattering of tsunami (Saito and Furumura 2009 [15]). Our 3-D N-S tsunami simulation simulates such all effects naturally and accurately.

3.1. Parallel FDM Simulation

For large scale FDM tsunami simulation, the 3-D model is partitioned horizontally (x,y) into subregions allocated to many processors for parallel computing and the MPI is used for inter-processor communications. The most consuming FDM simulation calculation of the 3-D N-S equation based on the SOLA algorithm appears in Eq. (7) for updating velocity and pressure components at individual cells together with surrounding cells iteratively at each time step. Such an iteration calculation sequence is, however, inefficient in extracting the power of the vector computing hardware such as employed in the ES.

We therefore used the T2K open supercomputer, a parallel computer having a large number of scalar processors connected over a fast interconnection network rather than using the ES vector supercomputer. The T2K has a shared-memory symmetrical multiprocessor (SMP) cluster architecture consists of four AMD Opteron scalar processors on each SMP node. Each has four processor cores with 2.2 GHz (16 cores on node). We here used a single-level flat MPI model in which single-threaded MPI processes are executed on each processor core.

The parallel simulation required computer memory of 50 GB and wall-clock time of 20 hours for tsunami propagation time of T = 8000 s using 400 processor cores (25

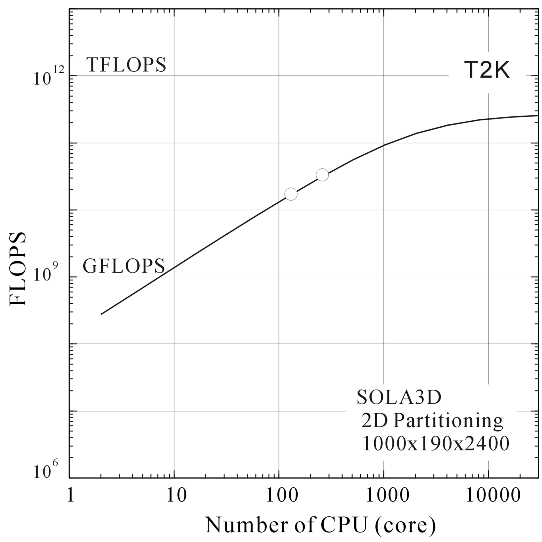

Fig. 5. Speed-up of parallel FDM simulation for 3-D tsunami propagation as a function of processor core numbers, estimated from parallel computing using 128 and 256 processor cores (open circles) and theoretical speed-up rate (solid line).

nodes) of the T2K.

We examined parallel simulation efficiency using large number of processor cores from 2 to 20,000 of the T2K supercomputer by measuring actual computation time using 128 and 256 processor cores (open circles, **Fig. 5**), and the theoretical parallel efficiency relative to time using 2 cores was estimated using the Amdahl' s law (**Fig. 5**, solid line). The present tsunami simulation code was not fully optimized for scalar processor architecture on the T2K, obtaining FDM simulation performance for the 3-D N-S equation of 0.14 GFLOPS per processor core, or just 1.5% of theoretical T2K performance at 9.2 GFOLOS/core. We need tune-up the present parallel code suitable to the architecture of the T2K scalar processor to achieve more large-scale tsunami simulations.

3.2. Simulation Model

3-D tsunami simulation model was 500 $\times$ 1200 km and 10 km deep, discretized into 1000 * 2400 * 100 grid points with a grid of 500 m horizontally and 100 m deep. We also used digital bathymetric data of J-EGG 500, provided by the Japan Oceanographic Data Center, in the tsunami simulation (**Fig. 6**).

Figure 7 illustrates coseismic seafloor displacement distribution derived by ground motion simulation for the 1944 Tonankai earthquake using the 3-D heterogeneous subsurface structure model for the Nankai-Trough subduction zone (**Fig. 7 (a)**) and that derived by using a homogeneous half-space model assuming rigid bedrock (Vp = 8 km/s, Vs = 4.6 km/s) (**Fig. 7**). Note that present tsunami simulation usually assumes such static seafloor elevation in a homogeneous half-space structure using a conventional computer code such as developed by Okada (1985) [16], rather than considering complex seafloor movement due to the actual 3-D heterogeneous structure.

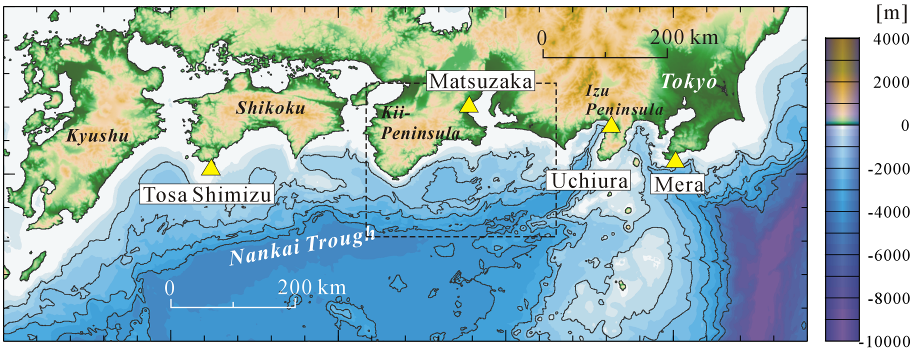

Fig. 6. Area of bathymetry for tsunami simulation of the 1944 Tonankai earthquake.

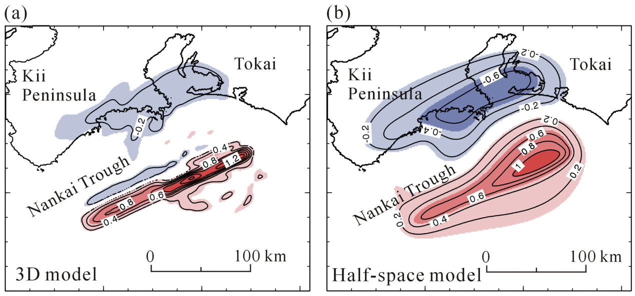

Fig. 7. Coseismic deformation of seafloor with uplift (red) and subsidence (blue) of seafloor derived in 3-D simulation of seismic wave propagation using (a) a 3-D heterogeneous structural model and (b) a homogeneous half-space model.

Sea floor elevation results due to low-angle thrust faulting at the top of the shallowly dipping (9 deg.) subducting Philippine-Sea Plate show large uplift in the seafloor along the trench of the Nankai Trough and subsidence of ground surface at the eastern coast of the Kii Peninsula. Such coseismic displacement distribution pattern derived by the 3-D model shows a large seafloor elevation in a relatively narrow zone about 20 km wide and 180 km long (**Fig. 7 (a)**). On the other hand the coseismic displacement pattern derived by simulation using the half-space model is spreading to the wider area of about 80 km and 200 km (**Fig. 7 (b)**). Maximum seafloor elevation derived by the 3-D and homogeneous half-space subsurface models is almost same at 1.2 m and 1.0 m, respectively. Such a wider seafloor tsunami source derived by the homogeneous half-space subsurface model (**Fig. 7 (b)**) should be developed for longer-period tsunamis compared to that derived from the 3-D model (**Fig. 6 (a)**), even though such steep and narrow seafloor elevation may be somewhat smoothed during tsunami generation process on the sea surface due to the low-cut filter effects of deep sea and finite source-rupture time (Kajiura, 1963 [13]; Saito and Furumura, 2008 [12]).

3.3. Simulation Results

The tsunami derived by the simulation for the 1944 Tonankai earthquake (**Fig. 8 (a)**, blue and red) at time T = 10, 20, 30, and 40 minutes after when the earthquake began had a tsunami wavefield for sea surface uplift and subsidence. The large slip at the northeastern part of the fault plane and fault rupture propagation from southwest to northeast produced large tsunamis eastward of the source region of the Tonankai earthquake. Some 10 minutes after the earthquake, a large tsunami arrived at the eastern Kii Peninsula and Tokai coast. As the tsunami propagated coastally, the tsunami height increases dramatically. Tsunamis over 2 m high hit the Pacific Ocean coast 10-20 min after the earthquake. Some 20 min after the earthquake the head of the tsunami had spread to the Izu Islands 300 km east of the hypocenter and to Cape Muroto in Shikoku, and by 40 min the tsunami propagated to the Boso Peninsula and Cape Shiono. As time passed, scattering of tsunami due to multiple reflections in heterogeneous bathymetry and around the islands modified the tsunami waveform very dramatically, leading to complex and long-term sea surface disturbances.

We compared tsunami simulation results for the 3-D N-S model to those from conventional tsunami simulation based on 2-D linear long-wave (LLW) theory. The LLW model effectively treats tsunamis in shallow seas with depth (H) less than the tsunami wavelength (L) ($H <$ 10-20*L). In our tsunami simulation for the LLW model, the initial tsunami for the sea surface elevation distribution is assumed to be identical to that of sea bottom elevation, which is also reasonable for considering tsunami generation in shallow seas with sea depth H less than 10 times of the sea bottom deformation area S_a ($H < 10*S_a$; Saito and Furumura, 2009 [12]). Note that the linear theory (Kajiura 1963 [13]) can also be used for more accurate estimation of initial tsunami distribution on the sea surface caused by the sea floor deformation in deep sea.

Results of tsunami simulation based on the 3-D N-S and the 2-D LLW models (**Figs. 8 (a)** and **8 (b)**) roughly correspond, but some discrepancy in tsunami waveform shape exists as the tsunami propagates longer distances. Dispersion of tsunami as it is propagating in relatively deep sea ($H >$ 4000 m) along the Nankai Trough produced long tsunami tails, which are clearly seen at T = 20 and 30 min frames for the 3-D N-S model (**Fig. 8 (a)**). Such dispersion property is not demonstrated in the tsunami simulation of the 2-D LLW model (**Fig. 8 (b)**), resulting in a simple tsunami head waves in all time frames. The tsunami simulated by the 2-D LLW model may therefore have overestimated initial tsunami height and under-

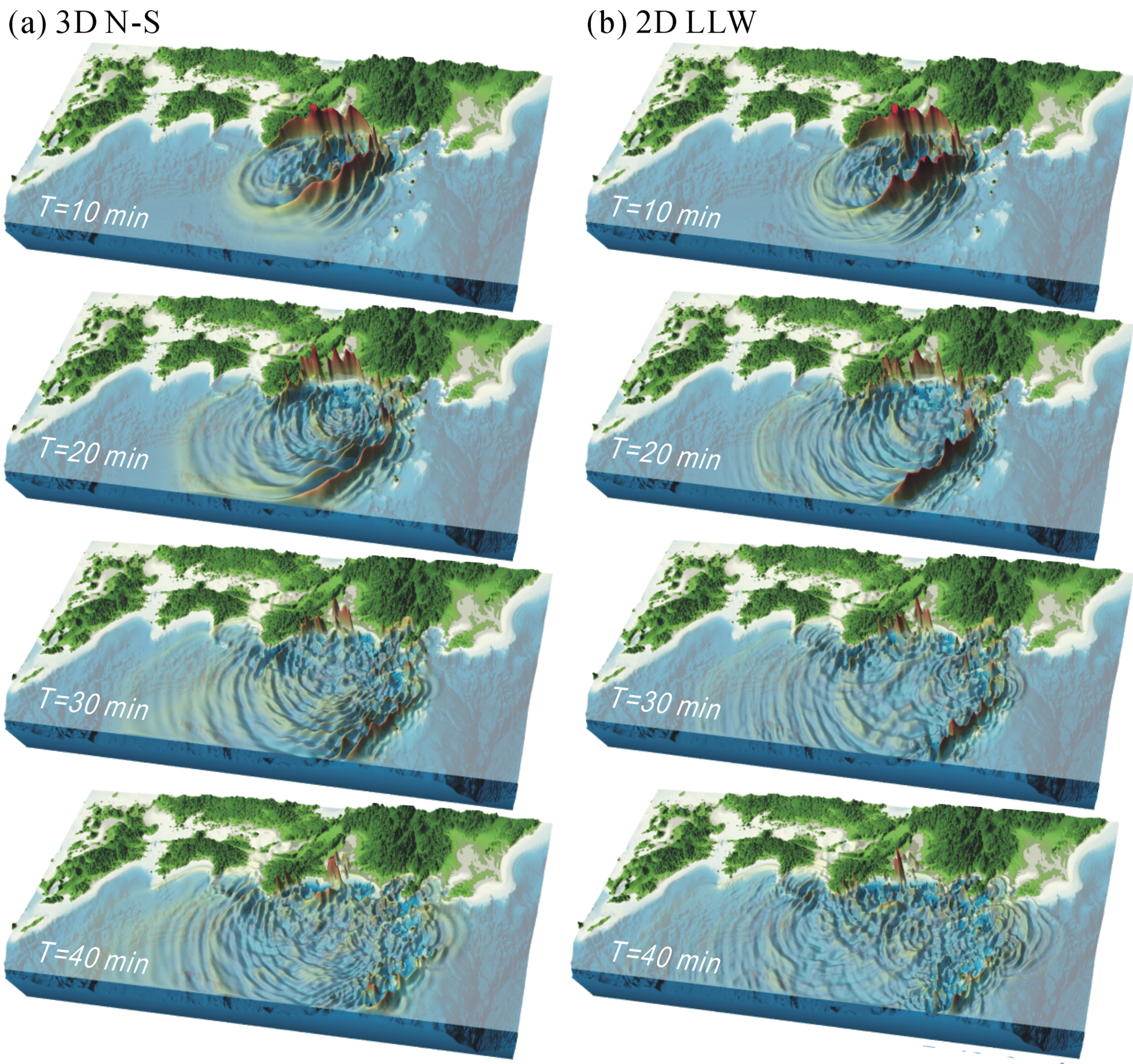

Fig. 8. Snapshots of tsunami at time T = 10, 20, 30, and 40 min from the source origin time derived in (a) 3-D N-S simulation and (b) the 2-D LLW model.

estimated duration time of distant tsunamis. Such discrepancies may be minor for tsunami at the coast of the Kii Peninsula and Tokai area because seas are shallow enough ($H < 2000$ m) to hold the LLW approximation.

We compare the simulated tsunami waveform derived by the integrated simulation of ground motion using a 3-D heterogeneous subsurface structural model and a homogeneous half-space model and tsunami simulation based on the 3-D N-S model and 2-D LLW model (**Fig. 9**). Simulated tsunami waveforms at Mera, Uchiura, Matsuzaka, and Tosa Shimizu stations (triangles, **Fig. 5**) have been applied a high-cut filter with a cut-off frequency of fc = 0.0167 Hz (cut-off period of $Tc = 1$ min) to remove high-frequency signals. The tsunami waveform derived by the half-space subsurface structure model (**Fig. 7 (b)**) shows a smooth, longer-wavelength tsunami compared to that from the heterogeneous 3-D structural model (**Fig. 7 (a)**) as is easily expected from the seafloor displacement distribution pattern shown in **Fig. 7**. Care is thus needed when using such tsunami waveforms as a Green function for tsunami source inversion.

The tsunami waveform derived by the simulation from the 3-D N-S model shows a somewhat smoother wave shape than that for the 2-D LLW model because the cover of thick sea water above the source acts high-wavenumber cut filter. A finite source-rupture time for the earthquake also removes large wave number components from the initial tsunami distribution on the sea surface. Some delay in tsunami arrival of 3-5 min in the 3-D N-S simulation in the tsunami record of distant Mera and Tosa Shimizu stations is due to the dispersion of tsunami propagating in deep Nankai Trough. Such effects are not accounted for in the 2-D LLW model.

The effectiveness of our 3-D N-S had also been demonstrated for the tsunami simulation of the 2004 M7.4 Off-Kii Peninsula earthquake in the Nankai Trough; the simulated dispersive tsunami waveform is well corresponding to the tsunami records of offshore cable tsunami sensors at Muroto Cape (Saito and Furumura (2009) [12]).

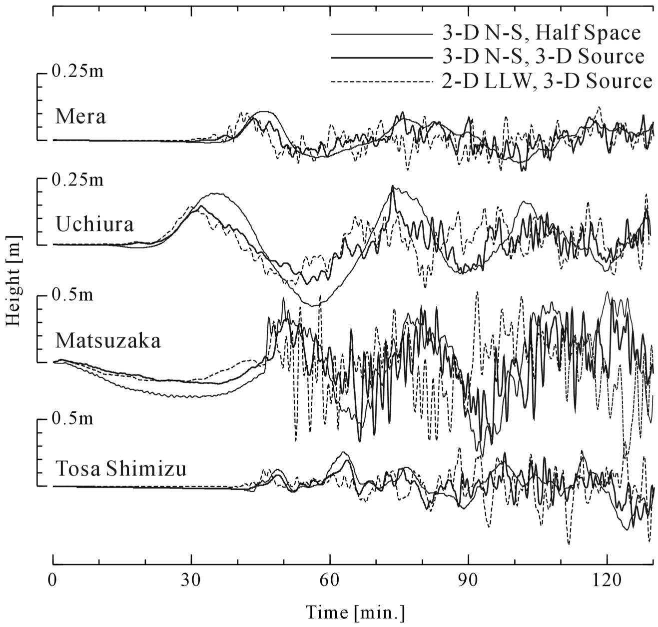

Fig. 9. Simulated tsunami waveform at Mera, Uchiura, Matsuzaka, and Tosa Shimizu (stations in **Fig. 5**) derived by simulation using 3-D N-S and source models assuming a 3-D heterogeneous structure (thick lines) (**Fig. 7 (a)**) and a homogeneous half-space model (thin lines) (**Fig. 7 (b)**) and 2-D LLW model (dashed lines).

4. Conclusions

Large (M $>$ 8) earthquakes occurring in the Nankai Trough might be causing significant disasters from Kyushu to Tokai along Japan's Pacific Ocean coast due to large, long-term ground shaking of long-period ground motions in sedimentary basins and tsunamis along the coastal zone. Coseismic vertical movements associated with large earthquakes also have caused rise and subsidence in coastlines near the source area. Downtown Kochi, Shikoku, sank after the 1946 Nankai earthquake due to coastal subsidence – exceeding 0.5 m. Such coseismic displacement is expected to cause additional coastal disasters with enhanced tsunami inundation and tidal wave effects.

To mitigate such earthquake-related disasters anticipated in future Nankai-Trough earthquakes, integrated ground motion and tsunami simulation using high-performance computers and reliable simulation models is indispensable. Our ground motion and tsunami simulation can be used to improve the accuracy of rapid fault parameters estimation for the Nankai-Trough earthquakes such as proposed by Imamura et al. (1991) [17]. Using present ES and T2K supercomputers, we have reproduced long-period ground motion, coseismic deformation, and tsunamis during the 1944 Tonankai earthquake very efficiently. Simulation and observation results agreed well for long-period ground motion developing in central Tokyo, indicating the effectiveness of the present simulation model for modeling long-period ($T > 2$ s) ground motion for the past and future earthquakes. At the moment we cannot directly compare simulated tsunami waveforms and observed onshore tide gauges tsunami records or tsunami height distributions, because the resolution of the present tsunami simulation of the 3-D N-S model is too coarse ($D = 200$ m) to evaluate dramatic amplification of tsunamis caused by shallow sea and complicated structures along coastlines. Anyhow, in order to demonstrate the effectiveness of our integrated simulation model for ground motion and tsunamis more clearly, we need conduct high-resolution simulation using a much denser ($D < 100$ m) mesh model.

In closing, we would like to note that tsunami and strong ground motion predictability depends both on computing power and on improvements in knowledge of the resolution of the simulation model for both heterogeneous subsurface structure and complex source-rupture process. We thus ensure that researchers in seismology and computer science work together to improve earthquake ground motion and tsunami simulation technology.

Acknowledgements

This study was supported by a grant-in aid from the Core Research for Evolutional Science and Technology (CREST), the Japan Science and Technology Agency, and the Research Project on "Improvements in strong ground motion and tsunami simulation accuracy for application of realistic disaster prevention of the Nankai Trough megathrust earthquake" of the Ministry of Education Culture and Sports and Technology of Japan. We thank personnel of the Earth Simulator Center, Japan Marine-Earth Science and Technology (JAMSTEC) for supporting CPU time of the Earth Simulator and to the Information Technology Center, the University of Tokyo, for supporting CPU time of the T2K Open Supercomputer. Constructive comments by two anonymous reviewers were greatly appreciated for revising manuscript.

References:

[1] T. Ohmachi, H. Tsukiyama, and H. Matsumoto, "Simulation of tsunami induced by dynamic displacement of seabed due to seismic faulting," Bull. Seism. Soc. Am., 91, pp. 1898-1909, 2001.

[2] T. Furumura, B. L. N. Kennettm and K. Koketsu, "Visualization of 3-D wave propagation from the 2000 Tottori-ken Seibu, Japan earthquake: Observation and numerical simulation," Bull. Seism. Soc. Am., 91, pp. 667-682, 2003.

[3] R. W. Graves, "Simulating seismic wave propagation in 3D elastic media using staggered-grid finite differences," Bull. Seism. Soc. Am., 86, pp. 1091-1106, 1996.

[4] C. Cerjan, D. Kosloff, R. Kosloff, and M. Reshef, "A nonreflecting boundary condition for discrete acoustic and elastic wave equations," Geophysics, 50, pp. 705-708, 1985.

[5] T. Furumura and L. Chen, "Large scale parallel simulation and visualization of 3D seismic wavefield using the Earth Simulator," Computer Modeling and Engineering Sciences, 6, pp. 143-168, 2004.

[6] Y. Tanaka, H. Miyake, K. Koketsu, T. Furumura, T. Hayakawa, T. Baba, T, H. Suzuki, and T. Masuda, "The DaiDaiToku integrated model of the velocity structure beneath the Tokyo metropolitan area (2)," Abst., Japan Geoscience Union Meet. 2006, S116-P014, 2006.

[7] T. Baba, A. Ito, Y. Kaneda, T. Hayakawa, and T. Furumura, "3D velocity structure model in the ocean around Japan inferred from controlled source seismic experiments," Abst., Japan Geoscience Union Meet. 2006.

[8] T. Furumura, T. Hayakawa, M. Nakamura, K. Koketsu, and T. Baba, "Development of long-period ground motions from the Nankai Trough, Japan, earthquakes: Observations and computer simulation of the 1944 Tonankai (Mw8.1) and the 2004 SE Off-Kii Peninsula (Mw7) Earthquakes," Pure Appl. Geophys., 165, pp. 585-607, 2008.

[9] Y. Yamanaka, "Source process of the 1944 Tonankai and the 1945 Mikawa earthquake," Chikyu Monthly, 305, pp. 739-745, 2004.

[10] T. Furumura and M. Nakamura, "Recovering of strong motion record of the 1944 Tonankai earthquake and long period ground mo-

tion in Kanto region," Geophysical Exploration, 59, pp. 337-351, in Japanese, 2006.
[11] C. W. Hirt, B. D. Nichols, and N. C. Romero, "SOLA – A numerical solution algorithm for transient fluid flows," Los Alamos National Laboratory report LA-5852, 1975.
[12] T. Saito and T. Furumura, "Three-dimensional simulation of tsunami generation and propagation: application to intraplate events," J. Geophys. Res., doi:10.1029/2007JB005523, 2009.
[13] K. Kajiura, "The leading wave of a tsunami," Bulletin of the Earthquake Research Institute, 41, pp. 545-571, 1963.
[14] Y. Shigihara and K. Fujima, "Wave dispersion effect in the Indian Ocean tsunami," Journal of Disaster Research, 1, 142 – 147, 2006.
[15] T. Saito and T. Furumura, "Scattering of linear long-wave tsunamis due to randomly fluctuating sea-bottom topography: coda excitation and scattering attenuation," Geophys. J. Int., 2008, in press.
[16] Y. Okada, "Surface deformation due to shear and tensile faults in a half space," Bull. Seismol. Soc. Am., 75, pp. 1135-1154, 1985.
[17] F. Imamura, Y. Izutani, and N. Shuto, "Accuracy of tsunami numerical forecasting with the rapid estimation method of fault parameters – A case of two fault planes with different stress drop of the 1944 Tonankai earthquake," Zisin 2, 44, 211-219, 1991.

Name:
Takashi Furumura

Affiliation:
Professor, Center for Integrated Disaster Information Research, Interfaculty Graduate School of Interdisciplinary Information Studies, The University of Tokyo

Address:
7-3-1 Hongo, Bunkyo-ku, Tokyo 113-0033, Japan

Brief Career:
1992-2000 Research Associate, Associate Professor, Hokkaido University of Education
2000-2008 Associate Professor, Earthquake Research Institute, The University of Tokyo
2008-Professor, Center for Integrated Disaster Information Research, Interfaculty Graduate School of Interdisciplinary Information Studies, The University of Tokyo

Selected Publications:
• "Development of long-period ground motions from the Nankai Trough, Japan, earthquakes: Observations and computer simulation of the 1944 Tonankai (Mw8.1) and the 2004 SE Off-Kii Peninsula (Mw7) Earthquakes," Pure and Applied Geophysics, Vol.165, pp. 585-607, 2008.
• "Anomalous propagation of long-period ground motions recorded in Tokyo during the 23 October 2004 Niitgata-ken Chuetsu (Mw6.6) earthquake, Japan," Bull. Seism. Soc. Am., Vol.97, pp. 863-880, 2007.
"Parallel simulation of strong ground motions during recent and historical damaging earthquakes in Tokyo, Japan," Parallel Computing, Vol.31, pp. 149-165, 2005.

Academic Societies & Scientific Organizations:
• Seismological Society of Japan (SSJ)
• Japan Geoscience Union (JpGU)
• American Geophysical Union (AGU)

Name:
Tatsuhiko Saito

Affiliation:
Post-Doc Fellow, Center for Integrated Disaster Information Research, Interfaculty Graduate School of Interdisciplinary Information Studies, The University of Tokyo

Address:
7-3-1 Hongo, Bunkyo-ku, Tokyo 113-0033, Japan

Brief Career:
2002-2003 JSPS Research Fellow, Tohoku University
2004-2005 JSPS Research Fellow, Advanced Industrial Science and Technology
2006- Post Doc Fellow, Center for Integrated Disaster Information Research, Interfaculty Graduate School of Interdisciplinary Information Studies, The University of Tokyo

Selected Publications:
• "Three dimensional simulations of tsunami generation and propagation: application to intraplate events," Journal of Geophysical Research, doi:10.1029/2007JB005523 (in press).

Academic Societies & Scientific Organizations:
• Seismological Society of Japan (SSJ)
• Society of Exploration Geophysicists of Japan (SEGJ)